ELSEVIER

Journal of Structural Geology 27 (2005) 541–551

JOURNAL OF STRUCTURAL GEOLOGY

www.elsevier.com/locate/jsg

Displacement rates and average earthquake recurrence intervals on normal faults

A. Nicol[a,b,*], J.J. Walsh[a], T. Manzocchi[a], N. Morewood[a]

[a]*Fault Analysis Group, Department of Geology, University College Dublin, Belfield, Dublin 4, Ireland*
[b]*Institute of Geological and Nuclear Sciences, PO Box 30368, Lower Hutt, New Zealand*

Received 16 October 2003; received in revised form 30 July 2004; accepted 29 October 2004
Available online 25 January 2005

Abstract

The factors controlling fault displacement rates and average recurrence intervals are investigated using data for 274 faults from four extensional regions. Combining established earthquake scaling laws with fault length and displacement rate data permits estimation of average recurrence intervals for each of the regions. Broad positive correlations between fault length and displacement rate are attributed to the proportional scaling of earthquake slip and rupture length coupled with constant average recurrence intervals that are independent of fault length. Stochastic and numerical modelling results suggest that fault interaction (and location) and intrabasinal strain rate variations are the principal factors responsible for scatter in the relations between length and displacement rate of individual fault systems; migration of the locus of faulting and death of large faults could be important in other areas. Further analysis indicates that decreases in average recurrence intervals between fault systems arise principally due to increases in regional strain rates. A negative correlation between average recurrence interval and basinal strain rate is confirmed by independent estimates of typical recurrence intervals from paleoseismological studies, and support the notion that high strain rates are accommodated by faster moving faults rather than larger numbers of faults. Basin-wide strain rate and fault size are the primary controls on displacement rates and average recurrence intervals, with fault interaction and intrabasinal strain rates being important secondary factors.

Keywords: Fault displacement rates; Earthquake recurrence intervals; Strain rates

1. Introduction

Faults within the earth's upper crust generally grow and accumulate slip during earthquakes. In circumstances where faults remain active for millions of years they can accommodate hundreds or thousands of earthquakes (e.g. Stein et al., 1988; Walsh and Watterson, 1988; Cowie and Scholz, 1992; Jackson and Leeder, 1994; Nicol et al., 2005). The rate of fault-growth is dependent on the amount and distribution of slip[1] associated with, and the period of time between (i.e. the recurrence interval), earthquakes. Fault displacement rate is a measure of growth rate, which previous work suggests is a function of fault size (with larger faults growing faster than smaller ones), regional strain rates and fault interactions (Nicol et al., 1997; Wesnousky, 1999; Walsh et al., 2001).

Using displacement rate and fault length data for 274 faults from four extensional regions, complemented by stochastic and numerical modelling, we investigate the many factors that control the displacement rates and average recurrence intervals of faults over geological time scales, i.e. averaged over periods of time ranging from 60 ka to 7 Ma. Since our analysis supports the notion of average recurrence intervals that are, to a first approximation, independent of fault length for each study area, we present our consideration of the controlling factors of fault growth in terms of average recurrence interval, a measure that combines both

* Corresponding author. Correspondence address: Institute of Geological and Nuclear Sciences, PO Box 30368, Lower Hutt, New Zealand. Tel.: +64-4-5701444; fax: +64-4-5704600

E-mail addresses: a.nicol@gns.cri.nz (A. Nicol), john@fag.ucd.ie (J.J. Walsh).

[1] Here the term *slip* refers to the fault offset arising from an individual earthquake, while *displacement* refers to cumulative offset arising from multiple events.

0191-8141/$ - see front matter © 2005 Elsevier Ltd. All rights reserved.
doi:10.1016/j.jsg.2004.10.009

displacement rates and fault length. A feature of all of the faults studied is that their lengths were unchanged on the time scales examined, i.e. no lateral fault propagation occurred. Fault displacement rates, measured at the point of maximum displacement along each fault, can then be used to estimate the average recurrence intervals of the larger earthquakes on a fault, assuming that all earthquakes have slip–length ratios in accordance with established empirical scaling laws (Wells and Coppersmith, 1994). The notion of displacement accumulating during large earthquakes that rupture much of a fault surface provides a crucial link between faulting processes on earthquake (e.g. up to thousands of years) and geological timescales (e.g. tens of thousands to millions of years) and permits a first-order analysis of earthquake recurrence intervals. Although our estimates of average recurrence interval are sensitive to which of two end member earthquake population models (i.e. Characteristic or Gutenberg–Richter) is adhered to, the main findings of our study are not.

2. Data and methods

Average recurrence intervals of 274 faults have been estimated for periods of time ranging from ca. 60 ka to 7 Ma from two offshore (Timor and North seas, with 101 and 129 faults respectively) and two partly onshore (Aegean and Taupo Rift, with 28 and 16 faults respectively) extensional terrains. Published fault lengths and displacement rates from the Timor Sea (Nicol et al., 1997; Meyer et al., 2002; Walsh et al., 2002), Inner Moray Firth in the North Sea (Nicol et al., 1997; Walsh et al., 2003a), the Gulf of Corinth region of the Aegean (Doutsos and Poulimenos, 1992; Armijo et al., 1996; Goldsworthy and Jackson, 2001; Morewood and Roberts, 2002; Micarelli et al., 2003) and Taupo Rift in the North Island of New Zealand (Villamor and Berryman, 2001; this study) form the basis for this paper. For the Timor Sea, North Sea and Taupo Rift we present all available fault data, while for the Aegean only those faults recognised in two or more publications were utilized. In all cases we have aggregated lengths and displacements for segmented fault arrays. All faults are tectonic and provide vertical displacements of growth strata (Timor Sea, North Sea and Aegean) and topographic surfaces (Taupo Rift). The dataset includes faults that cover a size range of 2–3 orders of magnitude, with lengths and vertical maximum displacements of 400 m to 40 km (Fig. 1) and 2 to 7000 m, respectively. Displacement rates for all faults range from 0.0003 to ca. 6 mm/yr (Fig. 1). Active faults are present in all regions except the North Sea where faulting is mid-late Jurassic in age (Walsh et al., 2003a).

In the two offshore examples, sedimentation rates exceed fault displacement rates. Accordingly, syn-faulting strata thicken across faults and record progressive fault displacements for up to five sedimentary intervals, each spanning 0.5–3 Ma. Data from these fault systems indicate that fault displacement rates were approximately uniform and that, in the North Sea and Timor Sea, fault lengths were near constant for much ($>80\%$) of the duration of faulting (Nicol et al., 1997; Meyer et al., 2002; Walsh et al., 2002, 2003a). Near-constant fault lengths have been suggested for the Aegean (Morewood and Roberts, 1999, 2002; Poulimenos, 2000) and can also be inferred for the sample period in the Taupo Rift where displacement rates reflect the last ca. 3–9% of the duration of extension and represent a snapshot of the evolution of the system.

The long-term stability of earthquake recurrence intervals is examined by plotting displacement rate as a function of fault length for the four extensional terrains (Fig. 1). As displacement rates on faults decrease towards their tips, we utilise the maximum displacement for the sample period. It would also be valid to use average displacements, although our results and general conclusions are not influenced by which of these measures are employed. Contours of recurrence interval of 100, 1000, 10,000 and 100,000 years are plotted on Fig. 1. In order to derive contours of recurrence interval we apply the empirical data of Wells and Coppersmith (1994) for the proportional scaling between coseismic slip (D_e) and earthquake rupture length (L_e); i.e. $D_e=(5\times10^{-5})L_e$. By assuming that each earthquake ruptured the entire fault length measured, and that all displacements arise from coseismic slip (i.e. no interseismic fault creep occurs on timescales of thousands of years), the displacement rate (D_{rate}) for a given recurrence interval (R_i) is equal to D_e/R_i or $(5\times10^{-5})L_e/R_i$. Thus, for a given recurrence interval it is possible to calculate displacement rates over a range of fault lengths or, alternatively, for a given displacement rate and fault length to determine an average recurrence interval.

Our analysis and derivation of recurrence intervals is most directly reconciled with the notion that each earthquake ruptures the entire fault length, and is therefore consistent with the Characteristic earthquake model for earthquake populations, in which a non power-law population is dominated by similar sized large earthquakes (Schwartz and Coppersmith, 1984; Wesnousky, 1994). Although faults do not always rupture in their entirety and multiple faults can slip in a single earthquake, even the Gutenberg–Richter earthquake model, which advocates a power-law scaling for earthquakes on an individual fault, demonstrates that slip during large earthquakes contributes a significant proportion of the total strain budget (Fig. 2). This is illustrated for a simple stochastic model in which a power-law, i.e. Gutenberg–Richter, population of earthquakes is randomly distributed over an elliptical fault surface. Earthquakes in the model have a constant earthquake-slip to rupture length ratio, consistent with established scaling relationships for earthquakes (Wells and Coppersmith, 1994), and the same normalised slip profile; the modelling results are, for the purposes of this article, insensitive to the slip–length ratio, a range of slip profiles (e.g. linear, elliptical, flat-topped) and the shape of the fault/

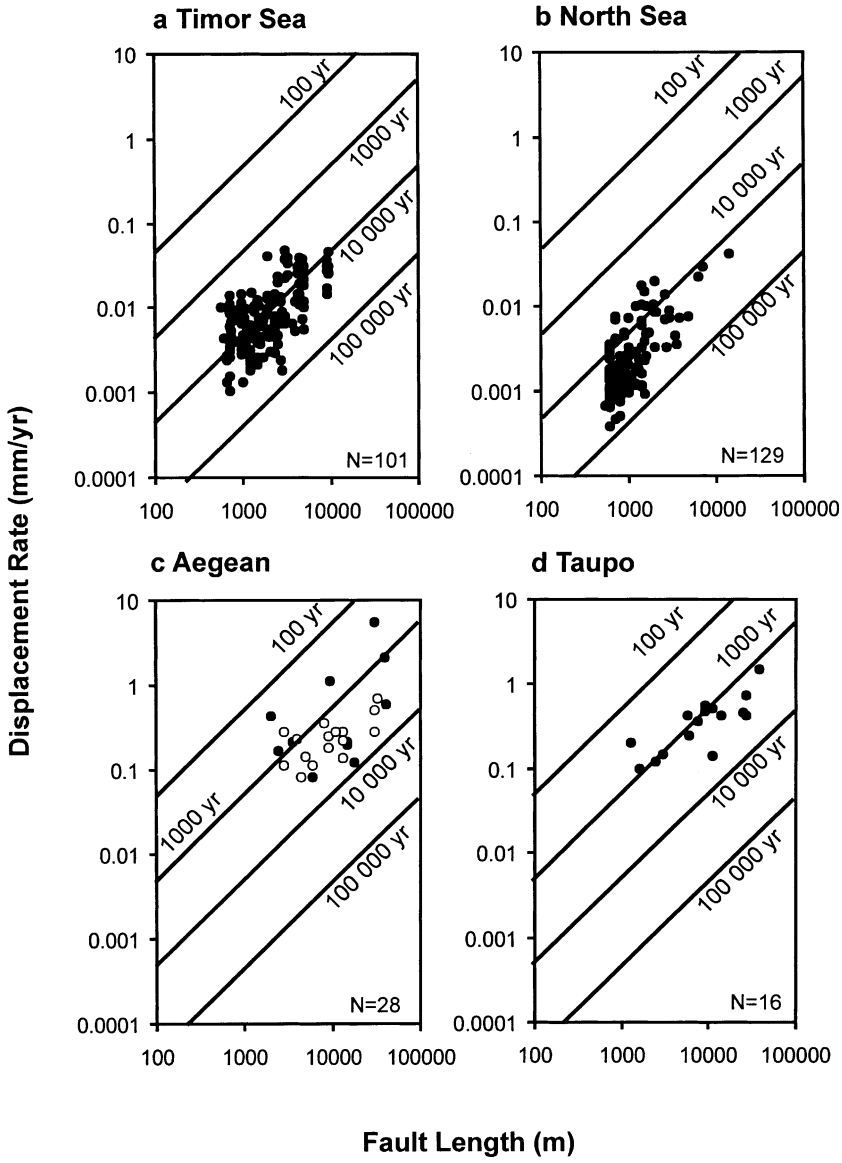

Fig. 1. Log–log plot of displacement rate against fault length for normal faults in two offshore, Timor Sea (a) and North Sea (b), and two partly onshore, Aegean (c) and Taupo Rift, New Zealand (d), regions. Faults in high strain (filled circles) and low strain (open circles) areas of the Aegean correspond to domains A and B of Poulimenos (2000), respectively. Domain A contains those faults considered to be most active (Goldsworthy and Jackson, 2001). For further details see text.

earthquake ruptures. For a 67-km-long fault generating a Gutenberg–Richter population of earthquakes with magnitudes up to 7 (Fig. 2a), the slip contribution of different sized earthquakes to the cumulative displacement at the centre of the fault (i.e. the point of maximum displacement) is strongly convergent, with 80% of the cumulative displacement arising from earthquakes with magnitudes greater than 6 (Fig. 2b). This cumulative displacement, however, is produced by 3.33 times as many earthquakes of magnitude $6<M<7$ in the Gutenberg–Richter model than would be required were it all accommodated by M7 earthquakes in the Characteristic model. Our estimates of recurrence times, based on the Characteristic earthquake model, will therefore be half of an order of magnitude greater than if they were based on the largest order of magnitude of earthquakes in a Gutenberg–Richter model.

Our consideration of earthquake scaling shows that it is possible to derive an acceptable estimate of the average recurrence intervals of the largest earthquakes on a fault, from the ratio of maximum earthquake slip to fault displacement rate, even when the earthquake population is Gutenberg–Richter. Since our estimates of recurrence interval, irrespective of whether a Characteristic or Gutenberg–Richter model is assumed, are invalidated in circumstances where fault lengths increase significantly on the time scales examined, we have analysed fault systems for which it has previously been demonstrated that fault lengths have remained approximately constant over the geological time

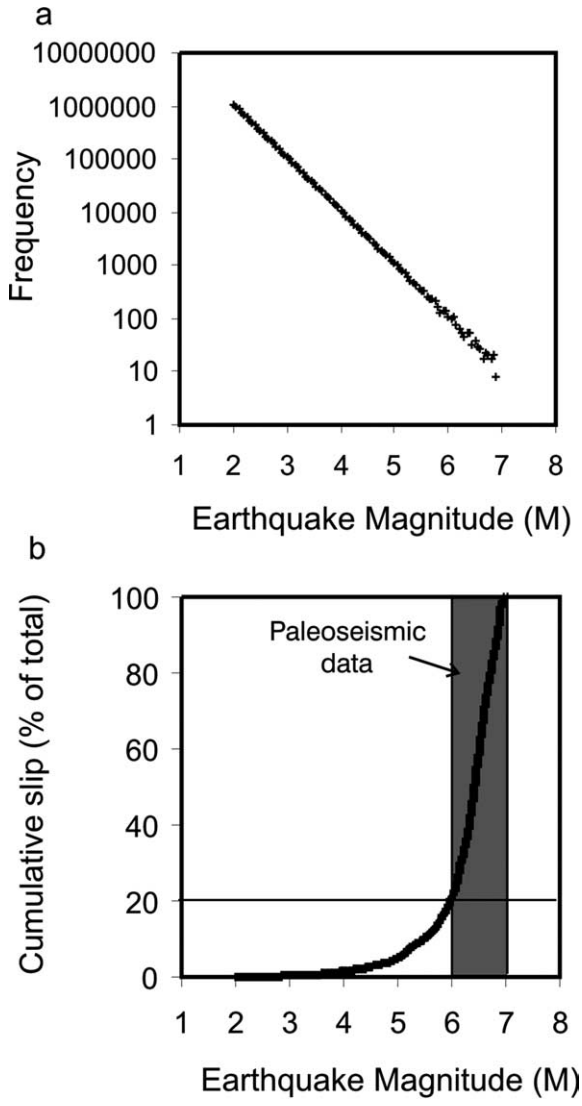

Fig. 2. Results from a stochastic model of earthquakes on an elliptical fault surface (aspect ratio of two) with a maximum dimension of 67 km parallel to fault strike. Earthquakes have elliptical rupture areas (at the same aspect ratio as the fault), semi-elliptical slip profiles, a ratio of maximum coseismic slip (D_c) to maximum rupture length (L_c) of 5×10^{-5} and the relationship $\log M_0 = 1.5M + 9.1$ linking moment and magnitude. Earthquakes are sampled from a Gutenberg–Richter ($2<M<7$) size distribution (a) and placed randomly in the fault ellipse. The slip events recorded at the centre of the fault are shown sorted according to the magnitude of earthquake from which they derive (b).

scales considered (Poulimenos, 2000; Meyer et al., 2002; Walsh et al., 2002; Childs et al., 2003; Walsh et al., 2003a). This type of behaviour, where fault lengths are near constant, is consistent with a recently developed fault growth model (Walsh et al., 2002). The principal advantage of our approach is that in circumstances where fault displacement rates are size dependent, as the available data suggests (see below), average recurrence interval provides a single measure of the rate dependency of the growth of a fault system; it also has the added advantage of permitting comparison with recurrence intervals independently estimated from paleoseismological studies utilizing trench and geomorphological data.

3. Estimation of average recurrence intervals

In each extensional terrain fault lengths and displacement rates range between 1 and 1.5 orders of magnitude (Fig. 1). Despite scatter of the data, the origins of which will be considered later, visual inspection suggests a broad positive relationship with larger faults tending to have higher displacement rates than smaller faults, consistent with previous studies from a number of regions of the globe and for different types of faults (Bilham and Bodin, 1992; Nicol et al., 1997; Wesnousky, 1999). Contours of average recurrence interval on Fig. 1, which were calculated independent of the data on this figure (see Section 2), have slopes of one and are parallel to the broad trends of the fault data. The near-proportional relationship between displacement rate and fault length in each dataset indicates that across a range of fault sizes in each region average recurrence intervals were, to a first approximation, constant with small faults experiencing earthquakes as frequently as large. Therefore, the most parsimonious interpretation of the data is that increases in displacement rate with fault size were mainly achieved by increases in the amount of coseismic slip, with larger faults experiencing larger earthquakes. The suggestion of broadly stable average recurrence intervals is consistent with Fig. 3, which shows

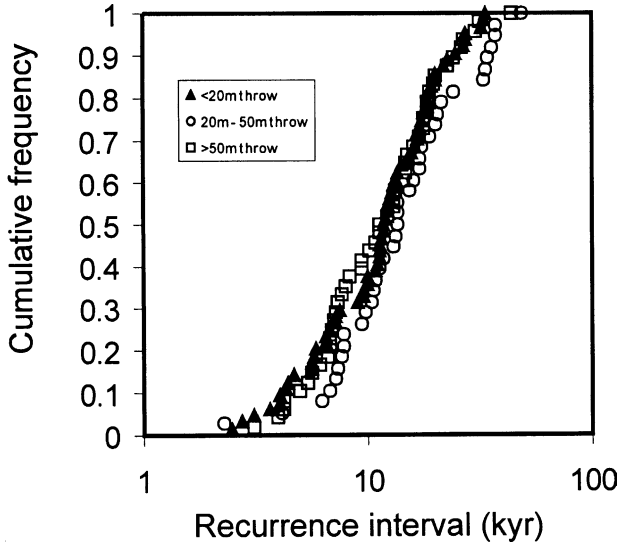

Fig. 3. Normalised cumulative distributions of recurrence intervals for all of the mapped faults in the Timor Sea dataset (Meyer et al., 2002). Average recurrence intervals are subdivided into three groups for faults with throws of <20 m ($n=64$), 20–50 m ($n=38$), and >50 m ($n=48$). Average recurrence intervals for the largest 23 faults (throw >20 m) have been calculated, where possible, over four periods during basin extension (i.e. multiple recurrence intervals have been measured for the largest faults), whilst the recurrence intervals for the remaining faults are averaged over their entire growth history. Data show that recurrence intervals are not dependent on fault size.

comparable average recurrence intervals for a wide range of fault sizes (20–180 m) over a period of 6 Ma in a fault system from the Timor Sea (Meyer et al., 2002). This result is unsurprising given the near-constant fault lengths and displacement rates for the Timor Sea dataset (Meyer et al., 2002; Walsh et al., 2002), which require that the distribution of data on Fig. 1a was maintained for much of the period of faulting. Although there is considerable variability in average recurrence intervals for individual faults in the system, there are no systematic differences in the distributions of average recurrence intervals for different size-classes of faults (Fig. 3).

4. Variations in average recurrence intervals

Although the available data highlight the importance of fault size (i.e. length) as a primary control on fault displacement rates, it is clear that variations in displacement rate for a given fault length occur both within, and between, datasets (Fig. 1). Within each fault system this variability is about one order of magnitude and partly reflects measurement errors which are typically $< \pm 20\%$ for both displacement rate and fault length. The scatter cannot, however, entirely be explained by measurement errors and in this section we consider the impact of a variety of geological factors, including fault interaction, fault linkage, fault death, intrabasinal variations in strain rate and fault strength.

4.1. Fault interaction

Fault interaction, with strain transfer between faults or strain shadow effects, will locally enhance or depress displacement rates (Ackermann and Schlische, 1997; Cowie, 1998; Cowie and Roberts, 2001; Walsh et al., 2001). This point is illustrated by the results of a numerical discrete element model from Walsh et al. (2001), which are presented in Fig. 4. The model shares many similarities with natural fault systems in that it comprises a number of parallel and non-uniformly spaced faults with a range of lengths and displacement rates. The model results indicate that although there is a general correlation between fault displacement rate and length, shorter faults located between the tips of large faults (e.g. Fig. 4 fault f) can have higher displacement rates than faults of a similar length that are centrally disposed relative to, and within the strain shadow of, large faults (e.g. Fig. 4 fault h). The elevated displacement rates on such faults may be achieved in a variety of ways, including a decrease in the recurrence interval or an increase in the slip to length ratio of the largest earthquakes. However the displacement rate changes are accommodated, it is clear that the locations of faults within an interacting fault network are an important control on fault displacement rates.

4.2. Fault linkage

Fault growth by segment linkage is thought by many to be an important process, in which originally isolated faults coincidentally overlap to form segmented fault arrays (e g. Trudgill and Cartwright, 1994; Cartwright et al., 1995; McLeod et al., 2000). By contrast, others argue that for many fault arrays the individual segments were kinematically interrelated from their initiation and may even link out-of-plane into a continuous fault (e.g. Mandl, 1987; Walsh et al., 2003b). In these circumstances fault segmentation occurs on well-defined scale ranges (typically with segment separations ≤ 1 km) and is simply a consequence of the propagation of individual faults through a rock volume (Mandl, 1987; Childs et al., 1995; Treagus and Lisle, 1997; Walsh et al., 2003b). The kinematic equivalence of fault segments is supported by earthquake studies demonstrating that individual earthquake events can be distributed across several segments, particularly towards the free surface (e.g. Wesnousky, 1988; Stewart and Hancock, 1991).

The origin of segmented fault arrays will be a critical determinant on fault displacement rates. The linkage of originally isolated faults might be expected to provide an increase in displacement rate, arising from the generation of a longer fault. By contrast, for models in which individual faults originally comprise an array of propagation-related soft-linked segments (i.e. bounded by relay ramps; Walsh et al., 2003b), fault length is equal to the total length of the array and hard linkage of previously soft linked segments should not increase displacement rates. An increase in the scatter in plots of displacement rate versus fault length would therefore only be expected where initially isolated faults link and where linkage occurs throughout the life of a fault system. For example, isolated faults that link late in the formation of a system will form a fault with lower average displacement rates than a fault of equal final length which linked during the early stages of faulting and accrued displacement at a rate commensurate with its increased length for a more significant proportion of the total period of fault system growth.

Although not a significant feature on the time scales considered for the four data sets included in our analysis, linkage of originally isolated faults could be important in other areas where the notion of near constant fault lengths is contravened. There is an increasing amount of evidence suggesting that this is most likely to occur during the earliest stages of the formation of a fault system, e.g. at relatively low strains of $<2\%$ (Meyer et al., 2002; Walsh et al., 2002). Similarly, for areas, or faults, in which the distinction between linkage of isolated faults and linkage of kinematically coherent segments is difficult to make, we would expect an increase in data scatter reflecting the subjective nature of this distinction; plotting three soft-linked fault segments as separate faults will provide a three-fold increase in displacement rate to length ratios. It is clear

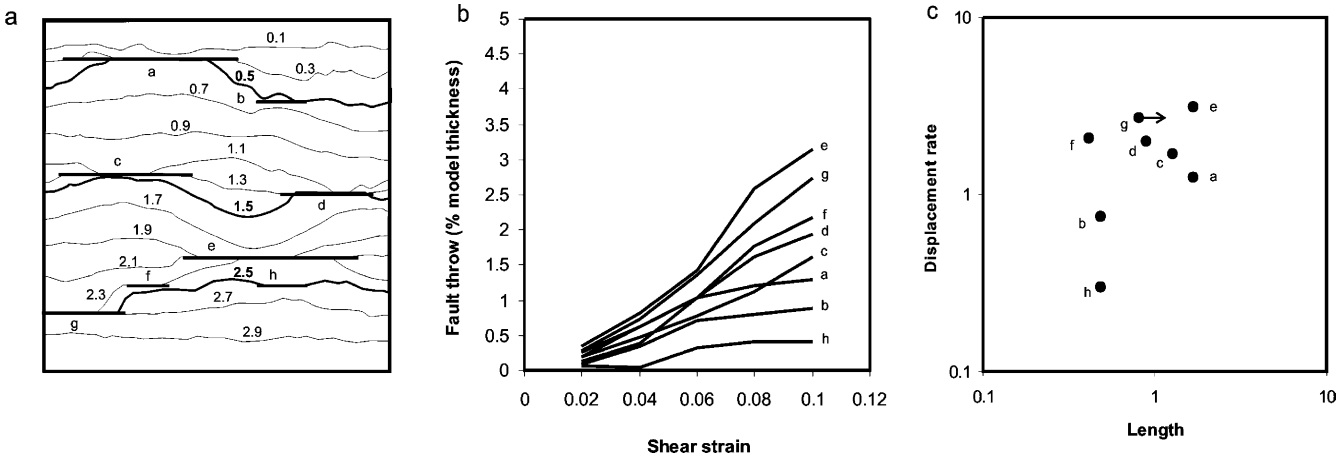

Fig. 4. (a) Fault map and (b) displacement rate–length relations for eight faults (labelled a–h) produced using a discrete element numerical model (Walsh et al., 2001). Model constructed with weak faults for a bulk shear strain of 0.3. Contours on (a) are in depth below a fixed datum on the top of the faulted cube. Fault g intersects the margin of the model and the measured length is a minimum (as indicated by the arrow). Refer to Walsh et al. (2001) for further details of the modelling and the text for discussion of the results.

therefore that, in common with displacement–length relationships for faults, failure to distinguish between fault segments and faults will increase the scatter on displacement rate to length data plots (Walsh et al., 2003b).

4.3. Fault death

As fault systems evolve the incremental strain budget may become progressively localized onto the largest faults (Nicol et al., 1997; Cowie et al., 2000; Meyer et al., 2002; Walsh et al., 2003a). Progressive strain localization is due mainly to the death of smaller faults, with the incremental strain they accommodated transferring to larger faults, and is another potential mechanism for introducing scatter in the plots of Fig. 1. To explore the impact of fault death on displacement rates of the large faults we analyse a synthetic fault system in which we impose systematic fault death (Fig. 5). The fault system was generated for a fault population with geometric characteristics similar to those of the Timor Sea study area (Nicol et al., 1997; Meyer et al., 2002; Walsh et al., 2002). The geometric model contains 1000 faults in an 88 km^2 region with lengths ranging from 170 to 10000 m (Fig. 5a) and a power-law length population of slope -1.7; a representative value in the range of slopes defined for natural fault datasets (-1.0 to -1.9; e.g. Watterson et al., 1996). The model is of a 10 Ma rifting event at a strain rate of 2×10^{-16} s^{-1}. The displacement rate of each active fault in the model is a linear function of its length, which is constant, and if all faults are active throughout the rifting event (Fig. 5d) they have a constant recurrence interval of ca. 9 ka (Fig. 5g). As the rifting progresses smaller faults are systematically terminated (i.e. killed off), whilst maintaining the same total strain rate. For the purposes of illustrating the impact of fault death on the displacement rates of the remaining active faults, the total length of active faults within the entire fault system was decreased at a linear rate (Fig. 5f). Fig. 5b and c shows maps of the active faults at 5 and 10 Ma; the very high mortality rates of faults within this simple model are chosen for illustrative purposes and are not typical of the fault system within the Timor Sea study area. The displacement accumulation on each fault was calculated during its entire period of activity (Fig. 5e), again assuming that the instantaneous displacement rate of each active fault is a linear function of its length.

Arising from the high slope of the fault length population and the high mortality rates, 999 faults die over the period of time between maps resulting in a 97.5% reduction in the total length of active faults and leaving just one active fault at the cessation of faulting (Fig. 5a–c). Although this rate of fault death is extreme, the strains previously accommodated by faults that died during growth of the model are small and as a consequence, displacement rates on the largest faults, averaged over their entire growth periods, only increase by 40% (Fig. 5g). The transfer of strain from small dead faults to the remaining active faults therefore produces only a minor shift of the data distribution in Fig. 5g which, given the scatter in the data from the natural systems (see above), is relatively unimportant. The small magnitude of the increase in displacement rates on the largest faults arises from the subordinate contribution of small faults to the total strain budget across the model and is significantly less than might be inferred by visual inspection of fault maps alone (e.g. compare Fig. 5a and c). Similar minor changes in displacement rate are typical of synthetic fault systems with the full range of population slopes (-1.0 to -1.9).

The above analysis considers displacement rates of faults averaged over the entire growth period of individual faults; a measure consistent with three of our datasets, in which either all, or a substantial part of, the growth of the fault system is examined. A greater increase in displacement rates approaching the conclusion of faulting would be observed on the remaining active faults if instantaneous, as

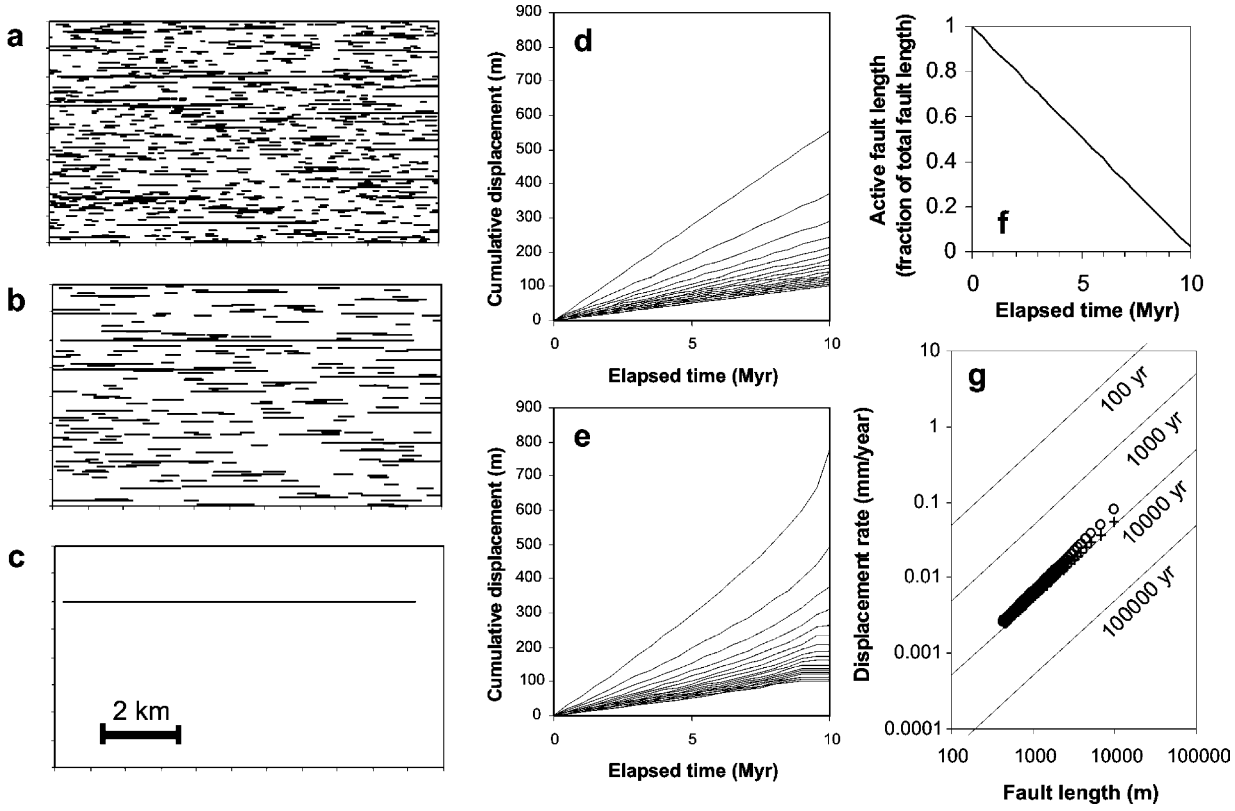

Fig. 5. Analysis of the impact of fault death on the displacement rates of the remaining active faults using a geometric model of fault system growth. (a)–(c) Show maps of active faults for a simple fault death model at time steps of 0 (a), 5 (b) and 10 Ma (c) during a 10 Ma rifting event. The model is for a fault system with geometric characteristics similar to those of the Timor Sea study area; constant fault lengths, an initial population of 1000 faults in an 88 km^2 region with lengths ranging from 170 to 10,000 m and a power-law length population of slope −1.7. (d) And (e) illustrate cumulative displacement versus time for the largest 20 faults in models excluding and including fault death, respectively. In the case of fault death (shown in (a)–(c)), the total active fault trace length decreases linearly as a function of time, with shorter faults dying first (f). A constant strain rate (2×10^{-16} s^{-1}) is maintained across the model by increasing the displacement rates of the larger, still active, faults. (g) Average displacement rates for cases including (circles) and excluding (plusses) fault death as a function of length. The labelled curves show contours of average recurrence interval (cf. Fig. 1). See text for further description of the models and discussion of the results.

opposed to average, rates were considered. Nevertheless, for a population in which small faults represent a significant component of the total number of faults (i.e. a slope of −1.7), the instantaneous displacement rates would only increase by a factor of four with the death of all but one fault.

4.4. Spatial and temporal variations in intrabasinal strain rate

In circumstances where strains are focused within a portion of an extensional basin and/or migrated between parts of the basin on timescales of hundreds of thousands of years, intrabasinal strain rates may vary (e g. Wallace, 1987; Jackson, 1999; Goldsworthy and Jackson, 2001). Changes in strain rates that are not accompanied by an adjustment in the number of active faults (see next section), are likely to be associated with a change in fault displacement rates, and could also contribute to the scatter of data in Fig. 1. For example, in the Gulf of Corinth region of the Aegean, the highest displacement rates occur on faults closest to the axis of the graben, in a region where total extension and the intrabasinal strain rates are also elevated (Poulimenos, 2000; Goldsworthy and Jackson, 2001). Consequently, faults in the high strain rate area (filled circles, Fig. 1c) typically have higher displacement rates for a given length than those in the low strain rate area (open circles, Fig. 1c). Late Quaternary fault data suggest that active deformation is focused close to the graben axis, which may indicate that the locus of activity has migrated basinward with time (Goldsworthy and Jackson, 2000, 2001). Such migration will only increase the scatter in Fig. 1 when it is accompanied by a change in the relative strain rates between areas.

4.5. Fault strength

The concept of fault strength, i e. whether a fault is weak or strong, is currently used in a variety of contexts. Fault strength can be an attribute of either fault rocks or individual faults, though direct equivalence is often assumed. From a geological perspective, ‘weak’ faults can be those that are characterised by high displacement rates and/or those that

are more likely to reactivate (Holdsworth et al., 1997; Imber et al., 1997; Walsh et al., 2001). In an earthquake context, 'weak' faults can be those that are more earthquake prone and/or are characterised by low stress drops (Scholz, 2000; Townend and Zoback, 2000; Zoback, 2000). Whatever the circumstances, faults that are weaker are often considered to have weaker fault rocks, either because they are inherently weaker, with, for example, low fault rock strength/frictional resistance, or because of some secondary factor such as elevated pore-fluid pressures (Holdsworth et al., 1997). This direct equivalence has, however, been questioned by recent studies suggesting that geometric aspects of a fault or fault system, such as fault size, location or connectivity, may be the main controls on long-term fault growth (Wesnousky, 1988; Stirling et al., 1996; Walsh et al., 2001). Although our data and numerical models provide direct evidence that geometric effects (i.e. fault length and location relative to other faults in the system) are important, they do not preclude the possibility that the long-term growth of the natural systems studied is to some significant extent controlled by either fault rock properties or pore-fluid pressures. For example, it could be argued that larger displacement faults have, on average, lower fault rock strengths or frictional properties, or are characterised by higher pore fluid pressures. There are, however, no data constraints on the spatial distributions of either fault rock properties or related pore-fluid pressures over a fault surface or for a fault system. In the absence of such data, the pre-eminence of fault rock properties for long-term fault growth cannot be tested. Instead, a combination of available quantitative data and numerical models suggests that geometric factors could, on their own, exercise the main control on fault growth on the time scales we have examined (Walsh et al., 2001). Even if this were the case, it is likely from both theoretical and observational constraints that the short term, earthquake, behaviour of faults will be sensitive to fault rock properties; e.g. for the same average displacement rate, lower fault rock strengths and higher related pore fluid pressures will lead to more, and smaller, earthquake events (Scholz, 1990). Our data and measures of average recurrence interval, although acceptable for the purposes of our article, cannot define, or even identify, these short-term differences in behaviour.

5. Impact of regional strain rates on recurrence intervals

Differences in displacement rates between data sets for faults of equal length range up to three orders of magnitude, which is significantly greater than the scatter within data sets. Data from each region occupy slightly different positions on Fig. 1 with geometric mean recurrence intervals for individual data sets of 1240 years (Aegean) to 22,350 years (North Sea). These inter-basin differences cannot be accounted for by measurement errors or local perturbations in fault growth, and point to a longer wavelength basin-wide control on fault kinematics and earthquake behaviour.

Nicol et al. (1997) document a positive relationship between fault displacement rates and regional strain rates and suggest that increases in strain rate are principally accompanied by increases in displacement rates rather than by a greater number of faults. This requires either a negative correlation between recurrence interval and strain rate, or a positive correlation between the ratio of coseismic slip to rupture length and strain rate. As there is no empirical or theoretical basis for suggesting that slip–length ratios increase with increasing strain rates, the most likely cause of the relationship between strain rate and displacement rates is a negative correlation between recurrence interval and strain rate. We examine the relations between average recurrence intervals and regional strain rates in Fig. 6 for six extensional terrains. Average recurrence intervals, assuming a constant ratio of coseismic slip to rupture length for each region were calculated using the geometric means of the data in Fig. 1. Strain rates were estimated from regional studies in the Aegean (Jackson and McKenzie, 1988; Clarke et al., 1997), the North Sea (Barr, 1985; Clausen et al., 1994), the Taupo Rift (Darby and Meertens, 1995; Villamor and Berryman, 2001) and the Timor Sea (Walsh et al., 1996). Comparison with independent estimates of typical recurrence intervals from paleoseismic trenching and geomorphic studies in the Aegean (Pantosti et al., 1996;

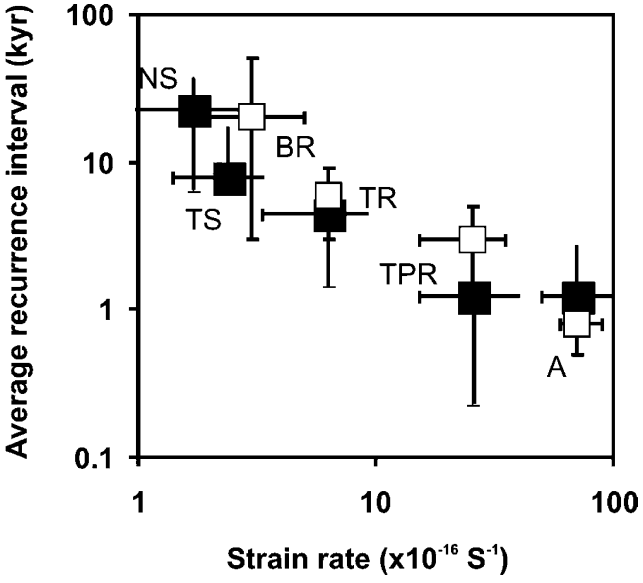

Fig. 6. Log–log plot of mean recurrence interval against regional strain rate for six extensional terrains; Basin and Range strain rate from Eddington et al. (1987); Dixon et al. (1995). Taranaki Rift strain rate and average recurrence interval (filled square) is from data in Thrasher et al. (1995); Nicol et al. (2004). Geometric means of recurrence intervals from the data in Fig. 1 are indicated by filled squares. Recurrence intervals for earthquakes of magnitudes 6–7 were estimated from paleoseismic studies and are shown by open squares (see text for further discussion). NS = North Sea, TS = Timor Sea, BR = Basin and Range, TR = Taranaki Rift, TPR = Taupo Rift, A = Aegean.

Collier et al., 1998; Koukouvelas et al., 2001; Pavlides et al., 2003), Taupo Rift (Villamor and Berryman, 2001; Villamor and Berryman, unpublished data, 2003), Basin and Range (Wallace, 1984) and the Taranaki Rift (Hull and Matsuda, 1981; Hull, 1994, 1996; Townsend, 1998) are also plotted in Fig. 6. This plot shows a near-proportional negative correlation (i.e. slope ~ -1) between average recurrence interval and strain rate, indicating that an order of magnitude increase in strain rate produces an order of magnitude decrease in average recurrence interval. The close match between the two independent sets of data implies that the assumption of a constant coseismic slip to rupture length ratio is appropriate to a first order; variability in the ratio amongst faults in the same system may be responsible for some of the scatter observed in Fig. 1, but imparts only a second-order effect on the primary dependency of strain rate on average recurrence interval. The primary underlying control on average recurrence intervals is therefore the rate at which a fault system was loaded. A corollary of these observations is that average recurrence intervals within a fault system may also change through time with adjustments in regional strain rates (Nicol et al., 2004).

Broad agreement of average recurrence intervals derived here and those measured in paleoseismic studies for the same basin provides some confidence in our analytical approach and the resulting conclusions. The similarity in these data supports the notion that large earthquakes, within an order of magnitude of the largest earthquake magnitude on a fault and, consequently, with rupture lengths no less than 30% of the fault length, account for most of the cumulative displacement on a fault. If this were not the case then many more smaller earthquakes would be required to achieve the same cumulative displacement and paleoseismological data, which generally only record events of magnitude 6 or greater, would tend to overestimate the size of recurrence intervals. Although both geological and paleoseismological evidence suggest that the average recurrence intervals of large earthquakes are related to regional strain rate, this long-term behaviour of recurrence intervals over a range of fault sizes is apparently at odds with many paleoearthquake studies for shorter periods of time (e.g. <20 ka). On time scales approaching that of the estimated recurrence interval (e.g. over a small number of earthquake cycles) there is often a high degree of temporal and spatial variability in earthquake recurrence (Wallace, 1987; Coppersmith, 1989; Sieh et al., 1989; Machette et al., 1991). These short-term fluctuations arise from the complex interactions of faults within critically stressed systems and constraints on the behaviour of fault systems on longer time scales is neither likely to assist in the accurate prediction of future earthquakes nor will it be of use for detailed assessment of earthquake hazard. Recognition of the independence of average recurrence interval and fault size is, however, relevant to a broader understanding of these issues.

6. Discussion and conclusions

Our analysis of the evolution of fault systems on geological time scales (e.g. 60 ka to multiple Ma) suggests that, on average, earthquake recurrence intervals in a particular fault system are, to a first approximation, constant for a range of fault sizes. Larger faults generally have higher displacement rates than smaller faults because they accommodate larger earthquakes with greater coseismic slip. This conclusion is not dependent on which earthquake population model, Gutenberg–Richter or Characteristic, is applied because in both cases larger earthquakes dominate the accumulation of displacement on faults; the resultant half an order of magnitude difference in recurrence interval between models is well below the variability observed between individual faults in the same fault system. Geological and paleoseismological estimates of recurrence interval support the notion that the primary underlying control on recurrence intervals is the rate at which a fault system is loaded, with increases in regional strain rates mainly accommodated by a reduction in average recurrence interval. These fault relations require that the number of large active faults in a system remains approximately stable, with increased strain rates accommodated by greater fault displacement rates rather than by the introduction of more large active faults. They also require that features such as fault interaction, fault linkage and fault zone strength provide controls on earthquake recurrence intervals that, on geological timescales, are subordinate to regional strain rate. These second-order factors may, however, provide important controls on the triggering and rupture-surface arrest of individual earthquakes.

These findings have been derived from the analysis of fault systems that, over the time scales examined, are not characterised by significant fault propagation or by the formation of new faults. Other types of fault systems may be characterised by more complex patterns of spatial and temporal evolution, though we still expect that the first order effects in all such cases will be an inverse relation between average recurrence interval and regional scale strain rate and the size dependence of fault displacement rates, with fault interaction and intrabasinal strain rate variations as important, though second order, factors.

Acknowledgements

This paper is the result of studies completed with financial support from the Royal Society of New Zealand Marsden Fund and from an Enterprise Ireland Basic Research Grant (SC/01/141). We thank other members of the Fault Analysis Group, in particular Conrad Childs and Juan Watterson, for discussions on fault-related growth issues, and Seth Stein and Tom Blenkinsop for their reviews.

References

Ackermann, R.V., Schlische, R.W., 1997. Anticlustering of small normal faults around larger faults. Geology 25, 1127–1130.

Armijo, R., Meyer, B.G.C.P., Rigo, A., Papanastassiou, D., 1996. Quaternary evolution of the Corinth Rift and its implications for the Late Cenozoic evolution of the Aegean. Geophysical Journal International 126, 11–53.

Barr, D., 1985. 3-D Palinspatic restoration of normal faults in the Inner Moray Firth: implications for extensional basin development. Earth Planetary Science Letters 75, 191–203.

Bilham, R., Bodin, P., 1992. Fault zone connectivity: slip rates and faults in the San Francisco Bay area, California. Science 258, 281–284.

Cartwright, J.A., Trudgill, B., Mansfield, C.S., 1995. Fault growth by segment linkage: an explanation for scatter in maximum displacement and trace length data from the Canyonlands Grabens of S.E. Utah. Journal of Structural Geology 17, 1319–1326.

Childs, C., Watterson, J., Walsh, J.J., 1995. Fault overlap zones within developing normal fault systems. Journal of the Geological Society, London 152, 535–549.

Childs, C., Nicol, A., Walsh, J.J., Watterson, J., 2003. The growth and propagation of syn-sedimentary faults. Journal of Structural Geology 25, 633–648.

Clarke, P., Davies, R.R., England, P.C., Parsons, B.E., Billiris, H., Paradissis, D., Veis, G., Cross, P.A., Denys, P.H., Ashkenazi, V., Bingley, R., 1997. Geodetic estimate of seismic hazard in the Gulf of Korinthos. Geophysical Research Letters 24, 1303–1306.

Clausen, O.-R., Korstgard, J.A., Petersen, K., McCann, T., O'Reilly, B.M., Shannon, P.M., Howard, C.B., Mason, P.J., Walsh, J.J., Watterson, J., 1994. Systematics of faults and fault arrays, in: Helbig, K. (Ed.), Modeling the Earth for Oil Exploration. Final Report of the CEC's Geoscience Program 1990–1993. Elsevier, pp. 205–316.

Collier, R., Pantosti, D., D'Addezio, G., De Martini, P.M., Masana, E., Sakellariou, D., 1998. Paleoseismicity of the 1981 Corinth earthquake fault: seismic contribution of extensional strain in central Greece and implications for seismic hazard. Journal of Geophysical Research 103, 30001–30020.

Coppersmith, K.J., 1989. On spatial and temporal clustering of paleoseismic events. Seismological Research Letters 59, 299–304.

Cowie, P.A., 1998. A healing–reloading feedback control on the growth rate of seismogenic faults. Journal of Structural Geology 20, 1075–1087.

Cowie, P.A., Scholz, C.H., 1992. Growth of fault by accumulation of seismic slip. Journal of Geophysical Research 97, 11085–11095.

Cowie, P.A., Gupta, S., Dawers, N.H., 2000. Implications of fault array evolution for synrift depocentre development: insights from a numerical fault growth model. Basin Research 12, 241–261.

Cowie, P.A., Roberts, G.P., 2001. Constraining slip rates and spacings for active normal faults. Journal of Structural Geology 23, 1901–1915.

Darby, D.J., Meertens, C.M., 1995. Terrestrial and GPS measurements of deformation across the Taupo back arc and Hikurangi forearc regions in New Zealand. Journal of Geophysical Research 100, 8221–8232.

Dixon, T.H., Robaudo, S., Lee, J., Reheis, M.C., 1995. Constraints on present-day Basin and Range deformation from space geodesy. Tectonics 14, 755–772.

Doutsos, T., Poulimenos, G., 1992. Geometry and kinematics of active faults and their seismotectonic significance in the western Corinth–Patras rift (Greece). Journal of Structural Geology 14, 689–699.

Eddington, P.K., Smith, R.B., Renggli, C., 1987. Kinematics of Basin and Range intraplate extension, in: Coward, M.P., Dewey, J.F., Hancock, P.L. (Eds.), Continental Extensional Tectonics Geological Society of London Special Publication, 28, pp. 371–392.

Goldsworthy, M., Jackson, J.A., 2000. Active normal fault evolution and interaction in Greece revealed by geomorphic and drainage patterns. Journal of the Geological Society of London 157, 967–981.

Goldsworthy, M., Jackson, J., 2001. Migration of activity within normal fault systems: examples from mainland Greece. Journal of Structural Geology 23, 489–506.

Holdsworth, R.E., Butler, C.A., Roberts, A.M., 1997. The recognition of reactivation during continental deformation. Journal of the Geological Society London 154, 73–78.

Hull, A.G., 1994. Past earthquake timing and magnitude along the Inglewood Fault, Taranaki, New Zealand. Bulletin of the New Zealand National Society for Earthquake Engineering 27, 155–162.

Hull, A.G., 1996. Earth and volcanic hazards in Taranaki: potential threats to oil and gas production and distribution infrastructure. In: 1996 New Zealand Petroleum Conference Proceedings, Ministry of Commerce, Wellington, pp. 261–271.

Hull, A.G., Matsuda, T., 1981. Late Quaternary faulting near Inglewood, North Island, New Zealand. In: Geological Society of New Zealand Annual Conference University of Waikato, Hamilton, 23–26 November, Abstracts 52.

Imber, J., Holdsworth, R.E., Butler, C.A., Lloyd, G.E., 1997. Fault-zone weakening processes along the reactivated Outer Hebrides Fault Zone, Scotland. Journal of the Geological Society London 154, 105–109.

Jackson, J., 1999. Fault death: a perspective from actively deforming regions. Journal of Structural Geology 21, 1003–1010.

Jackson, J., Leeder, M., 1994. Drainage systems and the development of normal faults: an example from Pleasant Valley, Nevada. Journal of Structural Geology 16, 1041–1059.

Jackson, J., McKenzie, D., 1988. Rates of deformation in the Aegean Sea and surrounding regions. Basin Research 1, 121–128.

Koukouvelas, I.K., Stamatopoulos, L., Katsonopoulou, D., Pavlides, S., 2001. A palaeoseismological and geoarchaeological investigation of the Eliki fault, Gulf of Corinth, Greece. Journal of Structural Geology 23, 531–543.

McLeod, A.E., Dawers, N.H., Underhill, J.R., 2000. The propagation and linkage of normal faults: insights from the Strathspey–Brent–Statfjord fault array, northern North Sea. Basin Research 12, 263–284.

Machette, M.N., Personius, S.F., Nelson, A.R., Schwartz, D.P., Lund, W.R., 1991. The Wasatch fault zone, Utah—segmentation and history of earthquakes. Journal of Structural Geology 13, 137–149.

Micarelli, L., Moretti, I., Daniel, J.M., 2003. Structural properties of rift-related normal faults: the case study of the Gulf of Corinth, Greece. Journal of Geodynamics 36, 275–303.

Mandl, G., 1987. Discontinuous fault zones. Journal of Structural Geology 9, 105–110.

Meyer, V., Nicol, A., Childs, C., Walsh, J.J., Watterson, J., 2002. Progressive localisation of strain during the evolution of a normal fault system in the Timor Sea. Journal of Structural Geology 24, 1215–1231.

Morewood, N.C., Roberts, G.P., 1999. Lateral propagation of the surface trace of the South Alkyonides fault, central Greece: its impact on models of fault growth and displacement–length relationships. Journal of Structural Geology 21, 635–652.

Morewood, N.C., Roberts, G.P., 2002. Surface observations of active normal fault propagation: implications for growth. Journal of the Geological Society of London 159, 263–272.

Nicol, A., Walsh, J.J., Watterson, J., Underhill, J.R., 1997. Displacement rates of normal faults. Nature 390, 157–159.

Nicol, A., Walsh, J.J., Berryman, K., Nodder, S., 2005. Growth of a normal fault by the accumulation of slip over millions of years. Journal of Structural Geology, in press.

Pantosti, D., Collier, R., D'Addezio, G., Masana, E., Sakellariou, D., 1996. Direct geological evidence for prior earthquakes on the 1981 Corinth fault (central Greece). Geophysical Research Letters 23, 3795–3798.

Pavlides, S., Koukouvelas, I., Ganas, A., Kokkalas, S., Tsodoulos, I., Stamatopoulos, L., Goyntromichou, C., Valkaniotis, S., 2003. Preliminary palaeoseismological results from the Kaparelli. European Geophysical Union Geophysical Research Abstracts, 07069.

Poulimenos, G., 2000. Scaling properties of normal fault populations in the western Corinth Graben, Greece: implications for fault growth in large strain settings. Journal of Structural Geology 22, 307–322.

Scholz, C.H., 1990. The Mechanics of Earthquakes and Faulting. Cambridge University Press, New York.

Scholz, C.H., 2000. Evidence for a strong San Andreas fault. Geology 28, 163–166.

Schwartz, D.P., Coppersmith, K.J., 1984. Fault behavior and characteristic earthquakes: examples from the Wasatch and San Andreas fault zones. Journal of Geophysical Research 89, 5681–5698.

Sieh, K.E., Stuiver, M., Brillinger, D., 1989. A more precise chronology of earthquakes produced by the San Andreas fault in southern California. Journal of Geophysical Research 94, 603–623.

Stein, R.S., King, G.C., Rundle, J.B., 1988. The growth of geological structures by repeated earthquakes. 2 Field examples of continental dip–slip faults. Journal of Geophysical Research 93, 13,319–13,331.

Stewart, I.S., Hancock, P.L., 1991. Scales of structural heterogeneity with neotectonic normal fault zones in the Aegean region. Journal of Structural Geology 13, 191–204.

Stirling, M.W., Wesnousky, S.G., Shimazaki, K., 1996. Fault trace complexity, cumulative slip, and the shape of the magnitude–frequency distribution for strike-slip faults: a global survey. Geophysical Journal International 124, 833–868.

Thrasher, G.P., King, P.R., Cook, R.A., 1995. Taranaki Basin Petroleum Atlas. 50 Maps plus Booklet. Institute of Geological and Nuclear Sciences Ltd, Lower Hutt.

Townend, J., Zoback, M.D., 2000. How faulting keeps the crust strong. Geology 28, 399–402.

Townsend, T., 1998. Paleoseismology of the Waverley fault zone and implications for earthquake hazard in South Taranaki, New Zealand. New Zealand Journal of Geology and Geophysics 41, 467–474.

Treagus, S.H., Lisle, R.J., 1997. Do principal surfaces of stress and strain always exist?. Journal of Structural Geology 19, 997–1010.

Trudgill, B., Cartwright, J., 1994. Relay ramp forms and normal fault linkages; Canyonlands National Park, Utah. Bulletin of the Geological Society of America 106, 1143–1157.

Villamor, P., Berryman, K., 2001. A late Quaternary extension rate in the Taupo Volcanic Zone, New Zealand, derived from fault slip data. New Zealand Journal of Geology and Geophysics 44, 243–269.

Wallace, R.E., 1984. Patterns and timing of late Quaternary faulting in the Great Basin Province and relation to some regional tectonic features. Journal of Geophysical Research 89, 5763–5769.

Wallace, R.E., 1987. Grouping and migration of surface faulting and variations in slip rates on faults in the Great Basin Province. Bulletin of the Seismological Society of America 77, 868–876.

Walsh, J.J., Watterson, J., 1988. Analysis of the relationship between the displacements and dimensions of faults. Journal of Structural Geology 10, 239–247.

Walsh, J.J., Watterson, J., Childs, C., Nicol, A., 1996. Ductile strain effects in the analysis of seismic interpretations of normal fault systems, in: Buchanan, P.G., Nieuwland, D.A. (Eds.), Modern Developments in Structural Interpretation, Validation and Modelling Geological Society of London Special Publication, 99, pp. 27–40.

Walsh, J.J., Childs, C., Manzocchi, T., Imber, J., Nicol, A., Meyer, V., Tuckwell, G., Bailey, W.R., Bonson, C.G., Watterson, J., Nell, P.A.R., Strand, J., 2001. Geometrical controls on the evolution of normal fault systems, in: Holdsworth, R.E. (Ed.), The Nature of the Tectonic Significance of Fault Zone Weakening Geological Society of London Special Publication, 186, pp. 157–170.

Walsh, J.J., Nicol, A., Childs, C., 2002. An alternative model for the growth of faults. Journal of Structural Geology 24, 1669–1675.

Walsh, J.J., Childs, C., Imber, J., Manzocchi, T., Watterson, J., Nell, P.A.R., 2003a. Strain localisation and population changes during fault system growth within the Inner Moray Firth, Northern North Sea. Journal of Structural Geology 25, 307–315.

Walsh, J.J., Bailey, W.R., Childs, C., Nicol, A., Bonson, C.G., 2003b. Formation of segmented normal faults: a 3-D perspective. Journal of Structural Geology 25, 1251–1262.

Watterson, J., Walsh, J.J., Gillespie, P.A., Easton, S., 1996. Scaling systematics of fault sizes on large scale range of fault map. Journal of Structural Geology 18, 199–214.

Wells, D.L., Coppersmith, K.J., 1994. New empirical relationships among magnitude, rupture length, rupture width, rupture area, and surface displacement. Bulletin of the Seismological Society of America 84, 974–1002.

Wesnousky, S.G., 1988. Seismological and structural evolution of strike-slip faults. Nature 335, 340–343.

Wesnousky, S.G., 1994. The Gutenberg–Richter distribution or characteristic earthquake distribution: which is it? Bulletin of the Seismological Society of America 84, 1940–1959.

Wesnousky, S.G., 1999. Crustal deformation processes and the stability of the Gutenberg–Richter relationship. Bulletin of the Seismological Society of America 89, 1131–1137.

Zoback, M.D., 2000. Strength of the San Andreas. Nature 405, 31–32.